

13. DATA REPORT: $^{40}\text{Ar}/^{39}\text{Ar}$ CHRONOLOGY OF DISCRETE ASH LAYERS IN THE NORTHWESTERN PACIFIC: ODP SITES 1149 AND 1179¹

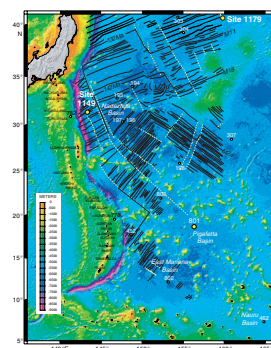
C. Escutia,² M. Canon,³ and J. Gutierrez-Pastor²

INTRODUCTION

Site 1149, drilled during Ocean Drilling Program (ODP) Leg 185, is located in the Nadezhda Basin southeast of Japan and ~100 km east of the Izu-Bonin Trench axis (Fig. F1). Site 1149 is located on magnetic Anomaly M11 (Nakanishi et al., 1992) with an assigned age of ~132 Ma (Gradstein et al., 1994, 1995; Plank, Ludden, Escutia, et al., 2000). The principal objective of Leg 185 was to determine the inputs into the Izu-Bonin Trench for “subduction factory” studies. Site 1179, on the abyssal seafloor ~1650 km east of Japan (Fig. F1), was drilled during ODP Leg 191. Site 1179 is located on magnetic Anomaly M8 (Nakanishi, et al., 1992) with an assigned age of 129 Ma (Gradstein et al., 1994, 1995). The main objectives of Leg 191 were to install a seismic monitoring station and to test the drilling and casing capabilities of the hard-rock re-entry system (“hammer drill”) (Kanazawa, Sager, Escutia, et al., 2001).

Despite the different scientific objectives of Legs 185 and 191, the sedimentary sections recovered from Sites 1149 and 1179 are the two most complete sections recovered from the northwestern Pacific Basin by either the Deep Sea Drilling Project (DSDP) (i.e., Legs 6, 20, 32, and 86) or ODP (i.e., Legs 185 and 191) (see Fig. F4 in Shipboard Scientific Party [2001]). During Leg 185, a complete sedimentary section (410 m) and an additional 133 m of highly altered volcanic basement were recovered. The Miocene to Pleistocene section (i.e., upper ~150 m) recovered from Site 1149 includes lithostratigraphic Unit I (0–118.2 meters below sea floor [mbsf]) and Subunit IIA (118.2–149.5 mbsf) of Plank,

F1. Site 1149 and 1179 locations, p. 9.



¹Escutia, C., Canon, M., and Gutierrez-Pastor, J., 2006. Data report: $^{40}\text{Ar}/^{39}\text{Ar}$ chronology of discrete ash layers in the northwestern Pacific: ODP Sites 1149 and 1179. In Ludden, J.N., Plank, T., and Escutia, C. (Eds.), *Proc. ODP, Sci. Results*, 185, 1–20 [Online]. Available from World Wide Web: <http://www-odp.tamu.edu/publications/185_SR/VOLUME/CHAPTERS/015.PDF>. [Cited YYYY-MM-DD]

²C.S.I.C.-Universidad de Granada. Instituto Andaluz de Ciencias de la Tierra, Campus de Fuentenueva, 18002 Granada, Spain.
Correspondence author:
cescutia@ugr.es

³Scandpower Petroleum Technology, 11490 Westheimer Road, Suite 500, Houston Texas 77082, USA.

Ludden, Escutia, et al. (2000) and consists of ash- and biogenic silica-bearing clay, radiolarian-bearing clay, silt-bearing clay, ash-bearing siliceous ooze, and diatomaceous clay, with numerous discrete volcanic ash layers (Plank, Ludden, Escutia, et al., 2000). During Leg 191, a near-continuous 375-m-thick sedimentary section was recovered in addition to 100 m of basaltic basement. The upper 221.5 m of the sedimentary section at Site 1179 (i.e., within lithostratigraphic Unit I of Kanazawa, Sager, Escutia et al. [2001]) consists of upper Miocene to Pleistocene clay- and radiolarian-bearing diatom ooze containing numerous discrete ash layers. The presence of discrete ash layers within the Miocene to Pleistocene sedimentary section at both Site 1149 and 1179 provides a unique opportunity to conduct $^{40}\text{Ar}/^{39}\text{Ar}$ ash chronology to refine the excellent magnetostratigraphic records (based on the scale of Berggren et al., 1995) obtained shipboard from both sites (Plank, Ludden, Escutia, et al., 2000; Kanazawa, Sager, Escutia, et al., 2001).

In this data report we present the analytical results from the $^{40}\text{Ar}/^{39}\text{Ar}$ incrementally heated analyses and provide a new combined late Miocene to Pleistocene $^{40}\text{Ar}/^{39}\text{Ar}$ and magnetostratigraphic chronology for the northwestern Pacific.

SAMPLE SELECTION AND ANALYTICAL METHODS

For this study, we reexamined all core sections from Sites 1149 and 1179 containing discrete ash layers (i.e., Cores 185-1149A-1H through 14H, 191-1179B-1H through 6H, and 191-1179C-2H through 17H) and identified a total of 94 discrete layers of vitric ash in the upper 120 m of the sedimentary column from Site 1149 and 16 discrete ash layers in the upper 190 m of the sedimentary column from Site 1179. In addition, many layers of clay were recognized, particularly at Site 1179, which may correspond with altered ash layers. These altered clay beds were not considered in this study.

Samples were taken from the discrete ash layers for smear slide examination and $^{40}\text{Ar}/^{39}\text{Ar}$ analyses. Smear slides were made to assess the approximate percentage of volcanic glass in the samples in order to determine their usefulness for $^{40}\text{Ar}/^{39}\text{Ar}$ analyses. Smear slide analyses showed the discrete ash layers at both sites to be mainly composed of well-sorted glass shards with few lithic fragments. Samples were selected for $^{40}\text{Ar}/^{39}\text{Ar}$ analyses based on (1) composition of ash layers (>60% of vitric glass, but commonly >80%), (2) their position in the stratigraphic column with respect to other ash beds, and (3) their position in the stratigraphic column with respect to the available ages derived from shipboard magnetostratigraphic studies (Tables T1, T2).

Samples were prepared and irradiated at the Oregon State University (OSU) (USA) Noble Gas Mass Spectrometry Laboratory. Detailed explanation about sample preparation and the irradiation process can be obtained from the OSU Web site: www.coas.oregonstate.edu/research/mg/chronology.html. In general, samples were sieved starting with the smallest size to remove detrital clays. The procedure started with a sieve opening of 63 μm . Most samples from Sites 1149 and 1179 were very clean glass shards and did not contain detrital clay. Those samples containing clay (i.e., Samples 185-1149A-12H-6, 79–80 cm, and 13H-3, 115–116 cm) were sieved incrementally increasing the sieve size opening until most of the clay was removed and a glass shard concentrate of

T1. $^{40}\text{Ar}/^{39}\text{Ar}$ analysis data, Site 1149, p. 15.

T2. $^{40}\text{Ar}/^{39}\text{Ar}$ analysis data, Site 1179, p. 16.

~95% was obtained. The samples were then washed, dried, and passed through a Frantz magnetic separator, followed by mild acid cleaning (HNO_3) for cleaning and final removal of detrital clay adhering to the glass shards. The concentrates were wrapped in copper foil, packaged in evacuated quartz vials, and irradiated in the OSU TRIGA reactor for 6 hr at 1 MW power. Reactor temperatures can reach 270°C. The neutron flux was measured using standard FCT-3 biotite (28.03 Ma) (Renne et al., 1994).

Values of the irradiation parameter J for individual sample packages were calculated by parabolic interpolation between the analyzed standards. After irradiation, milligram-sized fractions were spread on the bottom of 7-mm-diameter holes of a copper holder placed into an ultra high vacuum laser port and baked at 195°C for 48 hr during extraction line pump-down to $\sim 10^{-9}$ torr.

The samples were incrementally heated. Depending on sample composition, the incremental heating experiment may start at 200°–600°C and typically is complete by 1400°C using a Heine low-blank resistance furnace with a Ta/Nb crucible and Mo liner. Each heating step is 20 min duration with an additional 5 min cooling and continued removal of active gases with St101 Zr-Al and St172 Zr-V-Fe getters.

A MAP 215-50 rare gas mass spectrometer, source at 3000 V, equipped with a Johnston MM1-1SG electron multiplier at 2050 V was used for the analysis. During the 15-min analysis time per heating step, data are collected for 10 cycles of $m/z = 35$ –40 for baselines and peak tops. Data are reduced and age calculations completed using ArArCALC (version 2.2) for $^{40}\text{Ar}/^{39}\text{Ar}$ geochronology (Koppers, 2002), which for the age calculation includes the following decay constants:

$$\begin{aligned} & 5.543 \times 10^{-10} \text{ for the formation of } {}^{40}\text{Ar}, \\ & 2.94 \times 10^{-7} \text{ for the formation of } {}^{39}\text{Ar}, \\ & 8.23 \times 10^{-4} \text{ for the formation of } {}^{37}\text{Ar}, \text{ and} \\ & 2.303 \times 10^{-6} \text{ for the formation of } {}^{36}\text{Cl}. \end{aligned}$$

ANALYTICAL RESULTS

Results from the $^{40}\text{Ar}/^{39}\text{Ar}$ incrementally heated analyses are given in Figures F2, F3, F4, and F5 and in Tables T3 and T4. Complete data tables with additional data are provided (see “OSU-191” and “OSU-185” in the “Supplemental Materials” contents list).

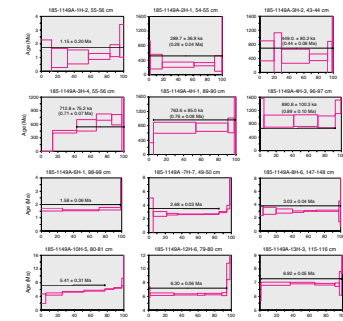
Site 1149

Age Spectra

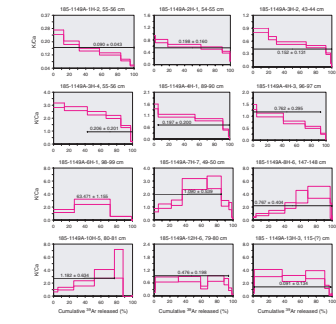
Figure F2 shows the age spectra for all Site 1149 samples listed in Table T3. The age spectra for Sample 185-1149A-1H-2, 55–56 cm, after a first step with broad ages ranging from ~0 to 2.28 Ma shows a progressive increase in ages from ~1.0 Ma to a final segment with a broad age range between ~1.02 and 3.4 Ma. The weighted plateau age is 1.15 ± 0.20 Ma, and the total fusion age is 1.12 ± 0.28 Ma.

The sample below (Sample 185-1149A-2H-1, 54–55 cm) exhibits a significantly younger age pattern, characterized by a broad age range in the first step (0–0.92 Ma) followed by a steady series of segments with ages between 0.28 and 0.36 Ma. The weighted plateau age is 0.28 ± 0.04 Ma, and the total fusion age is 0.31 ± 0.06 Ma.

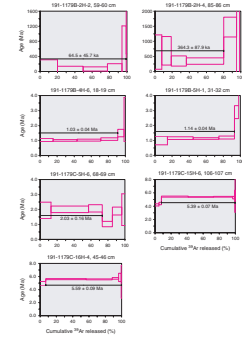
F2. Age spectra plots, Site 1149, p. 10.



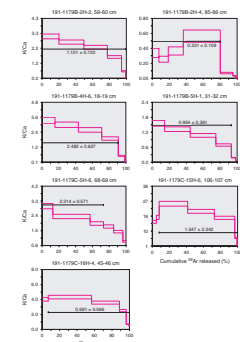
F3. K/Ca ratio plots, Site 1149, p. 11.



F4. Age spectra plots, Site 1179, p. 12.



F5. K/Ca ratio plots, Site 1179, p. 13.



Sample 185-1149A-3H-2, 43–44 cm, exhibits older ages than Sample 2H-1, 54–55 cm, and broad age ranges in all the steps (ranging from 0.42 to 0.81 Ma). The weighted plateau age is 0.44 ± 0.08 Ma, and the total fusion age is 0.502 ± 0.13 Ma.

Sample 185-1149A-3H-4, 55–56 cm, after a first step with age 0.0 ± 0.0 Ma, shows a series of segments with a progressive increase in ages from 0.43 to 0.76 Ma. The weighted plateau age is 0.71 ± 0.07 Ma, and the total fusion age is 0.69 ± 0.12 Ma.

Sample 185-1149A-4H-1, 89–90 cm, is characterized by a narrow younger age range first step followed by a steady series of segments with ages between 0.6 and 1 Ma. The weighted plateau age is 0.76 ± 0.08 Ma, and the total fusion age is 0.85 ± 0.10 Ma.

Sample 185-1149A-4H-3, 96–97 cm, is characterized by a broad range of older ages in the first step followed by a steady series of segments with ages between 0.65 and 1.05 Ma. The weighted plateau age is 0.89 ± 0.10 Ma, and the total fusion age is 0.96 ± 0.10 Ma.

Sample 185-1149A-6H-1, 98–99 cm, is characterized by a series of steady segments with narrow age ranges between 1.5 and 1.80 Ma. The weighted plateau age is 1.58 ± 0.06 Ma, and the total fusion age is 2.03 ± 0.07 Ma.

Sample 185-1149A-7H-7, 49–50 cm, is characterized by a first step with broad age range (0–5 Ma) followed by a steady series of narrower age segments ranging from ~2.5 to 3.0 Ma. The weighted plateau age is 2.68 ± 0.03 Ma, and the total fusion age is 3.11 ± 0.17 Ma.

Sample 185-1149A-8H-6, 147–148 cm, is characterized by a first step with ages ranging from ~2.45 to 3.75 Ma followed by a series of narrow steps with ages ranging from 2.9 to 3.1 Ma. The last step has broad ages ranging between 1.5 and 4.25 Ma. The weighted plateau age is 3.03 ± 0.04 Ma, and the total fusion age is 3.08 ± 0.12 Ma.

Sample 185-1149A-10H-5, 80–81 cm, exhibits a series of stepping narrow segments with increasing ages. The weighted plateau age is 5.41 ± 0.31 Ma, and the total fusion age is 5.56 ± 0.12 Ma.

Sample 185-1149A-12H-6, 79–80 cm, exhibits a first segment with a broad range in ages (5.75–7.25 Ma) followed by a series of steady segments with ages ranging between 6.25 and 6.50 Ma. The last segment exhibits an older and broader range of ages between 8.4 and 10.5 Ma. The weighted plateau age is 6.30 ± 0.06 Ma, and the total fusion age is 6.58 ± 0.09 Ma.

Sample 185-1149A-13H-3, 115–116 cm, exhibits a first step with a broad age range (5.75–6.75 Ma) followed by a steady series of segments with a narrow age range between 6.75 and 7 Ma. The last two segments exhibit broader age ranges between 6 and 7.5 Ma, and 7.5 and 9.0 Ma. The weighted plateau age is 6.92 ± 0.05 Ma, and the total fusion age is 7.02 ± 0.06 Ma.

K/Ca Ratios

Figure F3 shows the K/Ca variations for all samples; data are listed in Table T3. For most of the samples, there is a good correlation between the K/Ca ratio and the age spectra plots (Figs. F2, F3). Samples 185-1149A-1H-2, 55–56 cm; 2H-1, 54–55 cm; 3H-2, 43–44 cm; 3H-4, 55–56 cm; 4H-1, 89–90 cm; and 4H-3, 96–97 cm, display apparent maximum K/Ca ratio values in the lower temperatures and a monotonic decrease thereafter. Most of the remaining Leg 185 samples have higher K/Ca ratios at the mid-temperature steps (i.e., 700°–825°C) with a lower ratio at the lower and higher temperature steps. The K/Ca ratio values largely

T3. Incremental heating data, Site 1149, p. 17.

T4. Incremental heating data, Site 1179, p. 19.

overlap in Samples 185-1149A-2H-1, 54–55 cm, and 3H-2, 43–44 cm, which have decreasing values at higher temperatures (i.e., 0.873–0.119 and 0.843–0.021, respectively), and for sample 12H-6, 79–80 cm, with higher ratios at 825°C. Overlapping values are also observed in Samples 185-1149A-4H-1, 89–90 cm, and 4H-3, 96–97 cm, with higher ratios at the lower temperature steps (1.466 and 1.405, respectively) decreasing with higher temperatures to 0.058 and 0.071, respectively. Overlapping values of K/Ca ratios in Samples 185-1149A-3H-4, 55–56 cm; 6H-1, 98–99 cm; and 7H-7, 49–50 cm, show highest K/Ca ratios (i.e., 2.992, 2.804, and 2.894, respectively) at different temperature steps, and lower ratios are observed at the higher temperature steps. Samples 185-1149A-8H-6, 147–148 cm, and 10H-5, 80–81 cm, have overlapping K/Ca ratios with the highest values (i.e., 4.267 and 4.971, respectively) at the 900° and 800°C temperature steps, and lowest values at the higher temperature steps. K/Ca ratios in Samples 185-1149A-1H-2, 55–56 cm, and 13H-3, 115–116 cm, show no overlap with other samples. Sample 185-1149A-1H-2, 55–56 cm, exhibits a monotonic decrease in K/Ca ratio with the overall lowest values of all samples (i.e., 0.261–0.056).

Site 1179

Age Spectra

Figure F4 shows the age spectra for all Site 1179 samples, and data are listed in Table T4. The age spectra for Sample 191-1179B-2H-2, 59–60 cm, exhibits three steps of decreasing age ranging between 0 and 0.35 Ma, and two last steps of increasing ages with the last step showing a broad age range (0–1.2 Ma). The weighted plateau age is 0.06 ± 0.04 Ma and the total fusion age is 0.10 ± 0.70 Ma.

Sample 191-1179B-2H-4, 85–86 cm, has two first steps with broad range in ages (i.e., 0.1–1.25 Ma), followed by a steady set of steps with narrower age range between 0.25 and 0.40 Ma, and a last step with broad age spectrum ranging from 0 to 1.75 Ma. The weighted plateau age is 0.36 ± 0.09 Ma, and the total fusion age is 0.99 ± 0.18 Ma.

Sample 191-1179B-4H-6, 18–19 cm, exhibits a series of steady segments of narrow age spectra ranging between 1 and 1.25 Ma, and two last steps with ages ranging between 1.25 and 1.75 Ma, and 1.25 and 3.75 Ma, respectively. The weighted plateau age is 1.03 ± 0.04 Ma, and the total fusion age is 1.09 ± 0.04 Ma.

Sample 191-1179B-5H-1, 31–2 cm, exhibits a similar pattern of the age spectra to the last sample but with slightly older ages. The first step shows a broader range in ages between 0.75 and 1.25 Ma, followed by a series of steady segments with narrower age range (1–1.25 Ma), and the two last steps with an older and broader range in ages (i.e., 2.75–3.25 Ma). The weighted plateau age is 1.14 ± 0.04 Ma, and the total fusion age is 1.39 ± 0.06 Ma.

Sample 191-1179C-5H-6, 68–69 cm, exhibits a first step with broader age range between 1.40 and 2.50 Ma, followed by two segments with narrower range in ages (i.e., 1.75–2.25 Ma). The fourth segment of the age spectra exhibits a sudden decrease on the age range of the sample (i.e., 0.75–1.25 Ma) followed by the two last steps older ages. The weighted plateau age is 2.03 ± 0.16 Ma, and the total fusion age is 1.88 ± 0.14 Ma.

Samples 191-1179C-15H-6, 106–107 cm, and 16H-4, 45–46 cm, exhibit a similar pattern in their age spectra, characterized by a narrow range in ages in all steps. Both samples have broader range in ages in

the first step (i.e., 4–4.25 Ma and 4.25–5.25 Ma, respectively) followed by a series of steady segments with very narrow range in ages and ending with one or two segments with relatively broader range in ages (i.e., 5–5.30 Ma and 5.25–6.25 Ma, respectively). The weighted plateau age for Sample 191-1179C-15H-6, 106–107 cm, is 5.39 ± 0.07 Ma, and the total fusion age is 5.32 ± 0.07 Ma. The weighted plateau age for Sample 191-1179C-16H-4, 45–46 cm, is 5.59 ± 0.09 Ma, and the total fusion age is 5.56 ± 0.09 Ma.

K/Ca Ratios

Figure F5 shows the K/Ca variations for all samples, and data are listed in Table T4. For most of the samples, there is a good correlation between the K/Ca ratios and the age spectra plots (Figs. F4, F5). Only in Sample 191-1179C-15H-6, 106–107 cm, is the correlation not clear. Samples 191-1179B-2H-2, 59–60 cm; 4H-6, 18–19 cm; 5H-1, 131–132 cm; and 191-1179C-5H-6, 68–69 cm, display apparent maximum K/Ca ratio values in the lower temperatures and a monotonic decrease thereafter. The remaining samples show higher K/Ca ratio values at the 700–800°C temperature steps. Overlapping values are observed in Samples 191-1179B-2H-2, 59–60 cm; 4H-6, 18–19 cm; and 191-1179C-5H-6, 68–69 cm, with maximum K/Ca ratio values of 3.042, 3.345, and 3.015, respectively. Sample 191-1179C-15H-6, 106–107 cm, exhibits the highest K/Ca ratio observed in samples from both Sites 1149 and 1179, with maximum ratio values of 25.438 and minimum values of 1.143. Sample 191-1179B-2H-4, 85–86 cm, shows very low K/Ca ratio values between 0.563 and 0.003.

SIGNIFICANCE OF AGE SPECTRA RESULTS

Disturbed age spectra are common for argon data. Discordant $^{40}\text{Ar}/^{39}\text{Ar}$ age spectra can occur because the argon step-heating technique, resulting from the differential thermal stability of mineral phases during in vacuo heating, has the potential to separate different argon reservoirs hosted in varying mineralogical domains. The contribution of each separate mineral phase to the age spectra, however, may be monitored by elemental variations (Ca, Cl, and K from neutron-derived ^{37}Ar , ^{38}Ar , and ^{39}Ar , respectively). Meaningful interpretation of argon data, therefore, requires the support of petrographic and chemical analyses at a microscopic scale. High meaningless apparent ages in the low-temperature region such as those observed in Sample 185-1149A-4H-3, 96–97 cm, have also been observed in other argon step-heating analyses on volcanic rocks (e.g., Lo et al., 1994; Koppers et al., 2000). This was attributed to the lower release temperature of K-rich alteration mineral phases that may experience ^{39}Ar recoil loss during irradiation. High meaningless apparent ages in the high-temperature steps such as we observe (e.g., Samples 185-1149A-12H-6, 79–80 cm, and/or 191-1179B-5H-1, 31–32 cm) were also observed by Lo et al. (1994) and attributed to the release of argon from phenocrysts that may host extraneous argon (both inherited or excess argon). However, the intermediate region of the age spectra in our samples, attributed in previous studies to outgassing of glass and groundmass plagioclase by Lo et al. (1994) and of interstitials (glassy or microcrystalline) by Koppers et al. (2000), yield good plateau ages that are similar to the isochron ages (see “OSU-191” and “OSU-185” in the “Supplemental Ma-

terials" contents list). For this reason, despite the complicated release pattern, we consider the obtained ages meaningful.

Samples 185-1149A-4H to 13H and Samples 191-1179C-15H-6, 106–107 cm, and 191-1179C-16H-4, 45–46 cm, contain fair to good amounts of radiogenic ^{40}Ar , with some of the heating steps in each sample having ~50% or higher ^{40}Ar . The rest of the samples contain significantly lower percentages of radiogenic ^{40}Ar . The effect this low radiogenic ^{40}Ar has on the accuracy of the sample analysis is reflected in the larger uncertainty for these samples (e.g., 24% uncertainty for Sample 191-1149A-2H-4, 85–86 cm). The obtained ages follow, in general, both the stratigraphy of the sample groups (i.e., deeper samples give older ages at both sites) and the magnetostratigraphic ages obtained shipboard. Therefore, we consider that the ash beds from Sites 1149 and 1179 are dated with success.

Based on our obtained ages, the uppermost sample at Site 1149 (Sample 185-1149A-1H-2, 55–56 cm) yields an age older than the ash beds below. Although this age is clearly incompatible with its position in the stratigraphic column, the plateau and isochron are quite acceptable by analytical criteria. Thus, it is unlikely this result is due to sample contamination. Instead, either the glass contains "excess" ^{40}Ar that was not outgassed on eruption or the sample includes some older fragmental material that was incorporated in the eruption event. We prefer this last explanation for the older age since the isochron (see "OSU-191" and "OSU-185" in the "Supplemental Materials" contents list) shows no evidence of a younger age and a nonatmospheric $^{40}\text{Ar}/^{36}\text{Ar}$ intercept.

For most of the remaining samples, $^{40}\text{Ar}/^{39}\text{Ar}$ data yields, in general, internally consistent results based on correlation of the obtained $^{40}\text{Ar}/^{39}\text{Ar}$ ages with the shipboard magnetostratigraphic ages (Tables T1, T2). Few inconsistencies, however, are observed between the $^{40}\text{Ar}/^{39}\text{Ar}$ and the magnetostratigraphic ages. For example, older $^{40}\text{Ar}/^{39}\text{Ar}$ ages than those obtained by shipboard magnetostratigraphy in the same stratigraphic position are observed in Samples 185-1149A-10H-5, 80–81 cm; 191-1179B-4H-6, 18–19 cm; and 5H-1, 31–32 cm (Figs. F2, F4; Tables T1, T2). For Sample 191-1179C-5H-6, 68–69 cm, however, the $^{40}\text{Ar}/^{39}\text{Ar}$ age is consistent with the shipboard magnetostratigraphic age if we considered the uncertainty in the weighted plateau age (i.e., $2.03 + 0.16 = 2.19$ Ma).

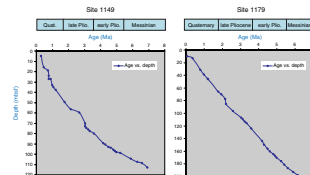
Based on the observations above, we summarize in Table T5 a new combined $^{40}\text{Ar}/^{39}\text{Ar}$ and magnetostratigraphic chronostratigraphy for the northwestern Pacific Sites 1149 and 1179. Age-depth plots for Sites 1149 and 1179 based in this new refined chronology are shown in Figure F6.

ACKNOWLEDGMENTS

We thank Dr. Paul Wallace for his review comments to this manuscript. This research used samples and/or data provided by the Ocean Drilling Program (ODP). ODP is sponsored by the U.S. National Science Foundation (NSF) and participating countries under management of Joint Oceanographic Institutions (JOI), Inc. Funding for this research was provided by two grants from the U.S. Science Support Program.

T5. Chronostratigraphy, p. 20.

F6. Age-depth plots, p. 14.



REFERENCES

- Berggren, W.A., Kent, D.V., Swisher, C.C., III, and Aubry, M.-P., 1995. A revised Cenozoic geochronology and chronostratigraphy. In Berggren, W.A., Kent, D.V., Aubry, M.-P., and Hardenbol, J. (Eds.), *Geochronology, Time Scales and Global Stratigraphic Correlation*. Spec. Publ.—SEPM (Soc. Sediment. Geol.), 54:129–212.
- Gradstein, F.M., Agterberg, F.P., Ogg, J.G., Hardenbol, J., van Veen, P., Thierry, J., and Huang, Z., 1994. A Mesozoic time scale. *J. Geophys. Res.*, 99:24051–24074.
- Gradstein, F.M., Agterberg, F.P., Ogg, J.G., Hardenbol, J., van Veen, P., Thierry, J., and Huang, Z., 1995. A Triassic, Jurassic and Cretaceous time scale. In Berggren, W.A., Kent, D.V., Aubry, M.P., and Hardenbol, J. (Eds.), *Geochronology, Time Scales and Global Stratigraphic Correlation*. Spec. Publ.—SEPM (Soc. Sediment. Geol.), 54:95–126.
- Lo, C.-H., Onstott, T.C., Chen, C.-H., and Lee, T., 1994. An assessment of $^{40}\text{Ar}/^{39}\text{Ar}$ dating for the whole-rock volcanic samples from the Luzon Arc near Taiwan. *Chem. Geol.*, 114:157–178.
- Kanazawa, T., Sager, W.W., Escutia, C., et al., 2001. *Proc. ODP, Init. Repts.*, 191 [CD-ROM]. Available from: Ocean Drilling Program, Texas A&M University, College Station TX 77845-9547, USA. [[HTML](#)]
- Koppers, A.A.P., 2002. ArArCALC: software for $^{40}\text{Ar}/^{39}\text{Ar}$ age calculations. *Comput. Geosci.*, 28:605–619.
- Koppers, A.A.P., Staudigel, H., and Wijbrans, J.R., 2000. Dating crystalline groundmass separates of altered Cretaceous seamount basalts by the $^{40}\text{Ar}/^{39}\text{Ar}$ incremental heating technique. *Chem. Geol.*, 166:139–158. doi: [10.1016/S0009-2541\(99\)00188-6](https://doi.org/10.1016/S0009-2541(99)00188-6)
- Nakanishi, M., Tamaki, K., and Kobayashi, K., 1992. Magnetic anomaly lineations from Late Jurassic to Early Cretaceous in the west-central Pacific Ocean. *Geophys. J. Int.*, 109:701–719.
- Plank, T., Ludden, J.N., Escutia, C., et al., 2000. *Proc. ODP, Init. Repts.*, 185 [CD-ROM]. Available from: Ocean Drilling Program, Texas A&M University, College Station TX 77845-9547, USA. [[HTML](#)]
- Renne, P.R., Deino, A.L., Walter, R.C., Turrin, B.D., Swisher, C.C., Becker, T.A., Curtis, G.H., Sharp, W.D., and Jaouni, A.-R., 1994. Intercalibration of astronomical and radioisotopic time. *Geology*, 22:783–786.
- Shipboard Scientific Party, 2001. Leg 191 summary. In Kanazawa, T., Sager, W.W., Escutia, C., et al., *Proc. ODP, Init. Repts.*, 191, 1–49 [CD-ROM]. Available from: Ocean Drilling Program, Texas A&M University, College Station TX 77845-9547, USA. [[HTML](#)]

Figure F1. Location of Site 1149 drilled during Leg 185 and Site 1179 drilled during Leg 191. Also shown are the magnetic lineations in the northwestern Pacific.

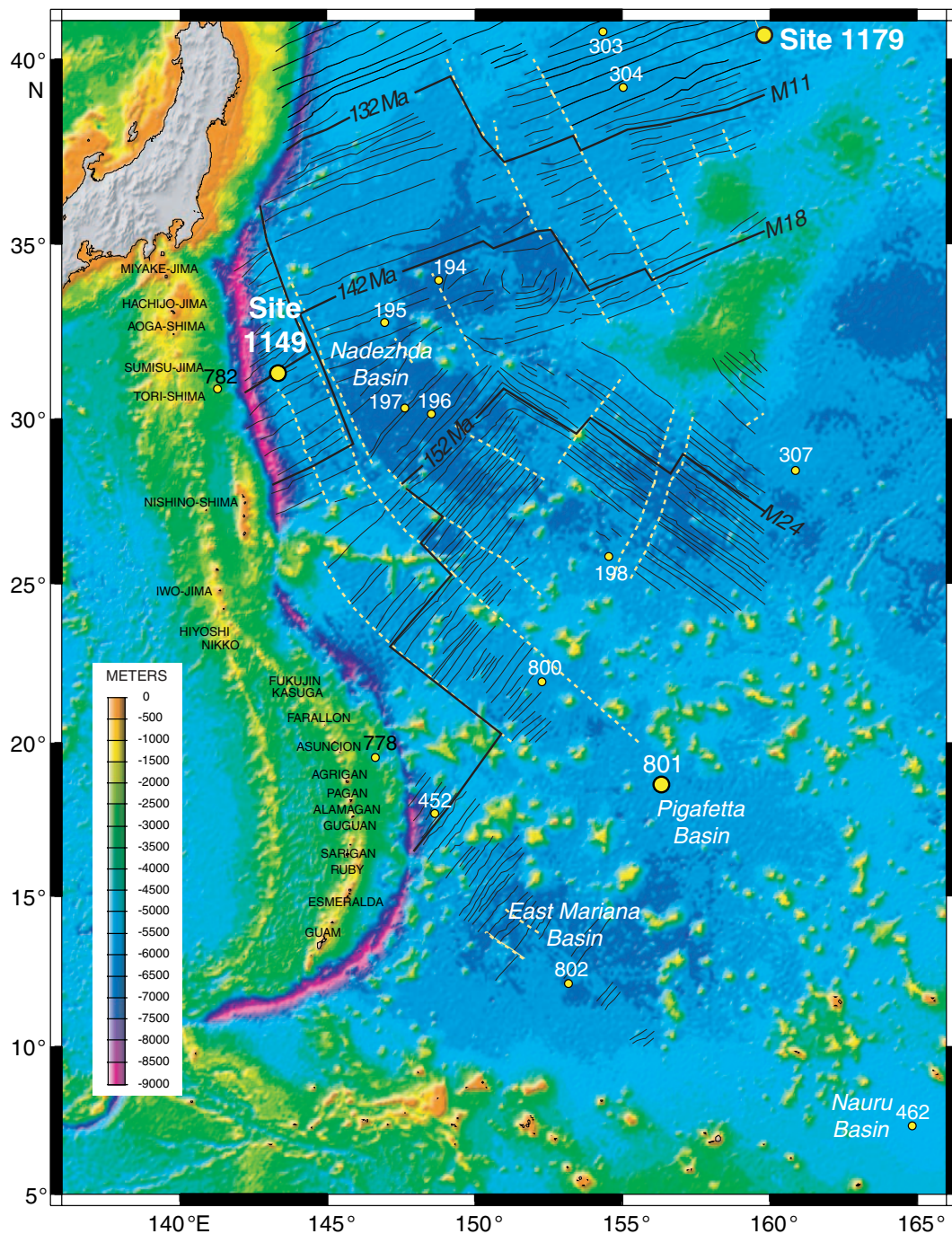


Figure F2. Argon-release age spectra plots for Site 1149 samples. Black lines = weighted plateau ages.

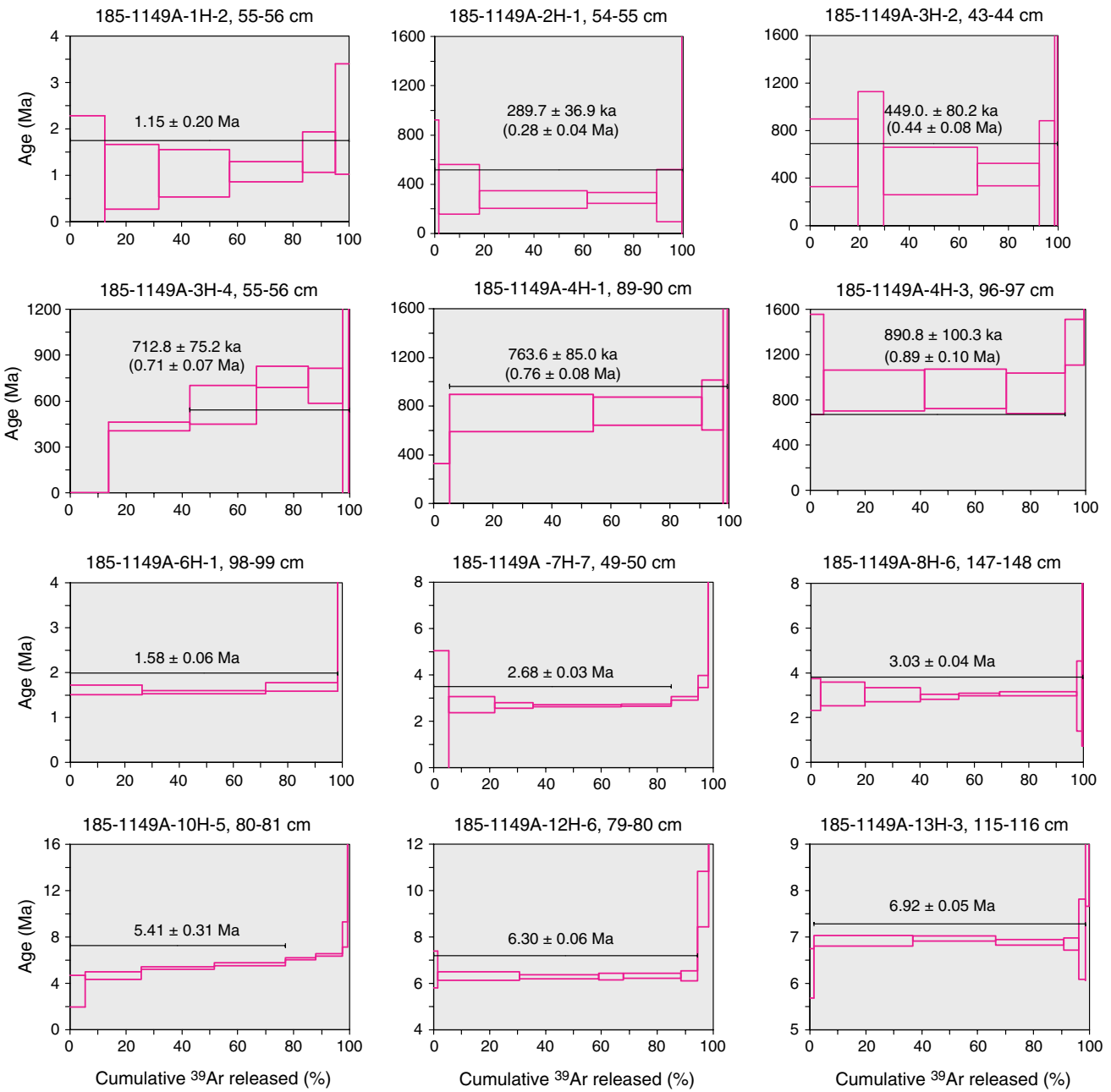


Figure F3. K/Ca ratio plots for Site 1149 samples.

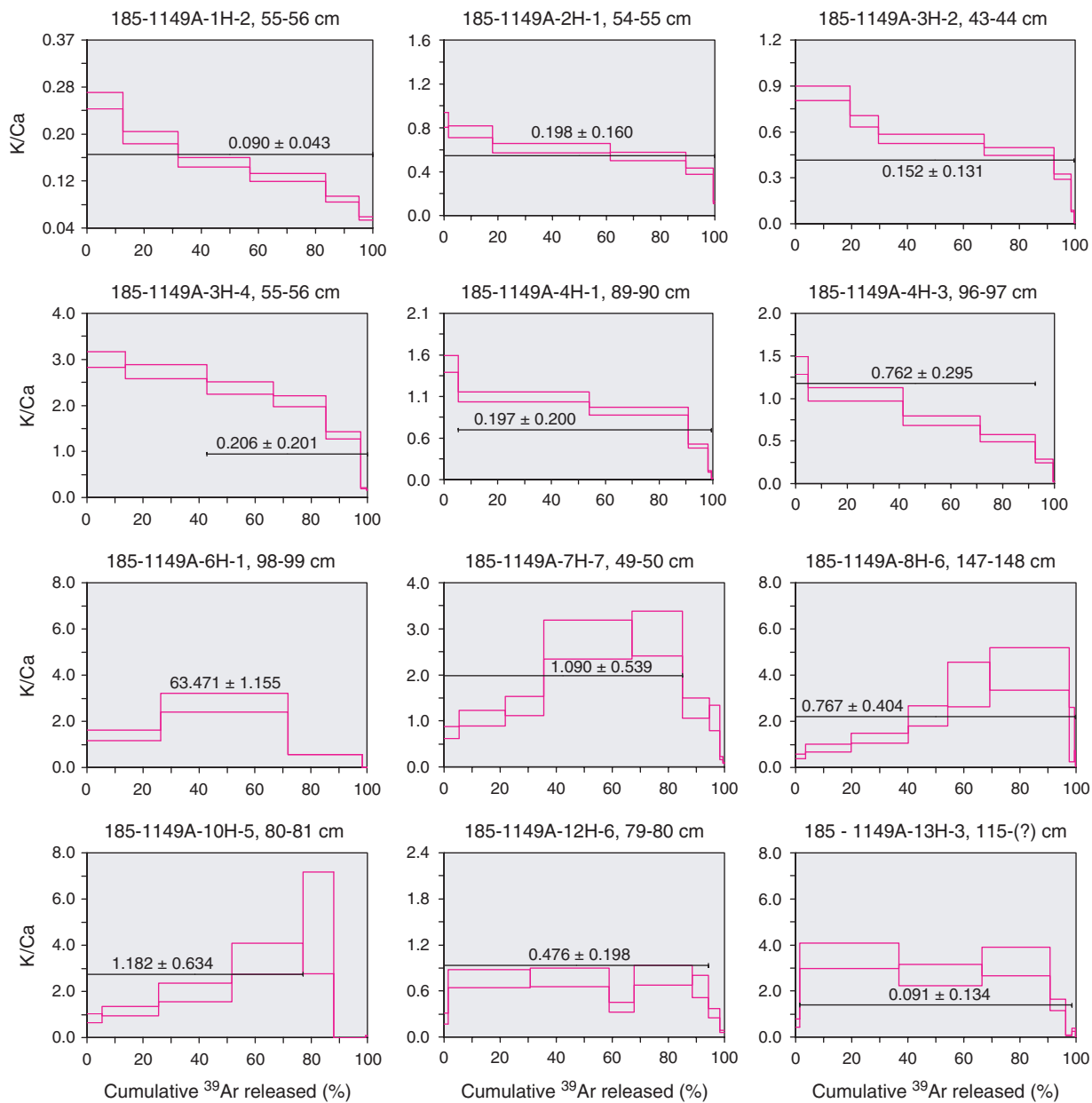


Figure F4. Argon-release age spectra plots for Site 1179 samples. Black lines = weighted plateau ages.

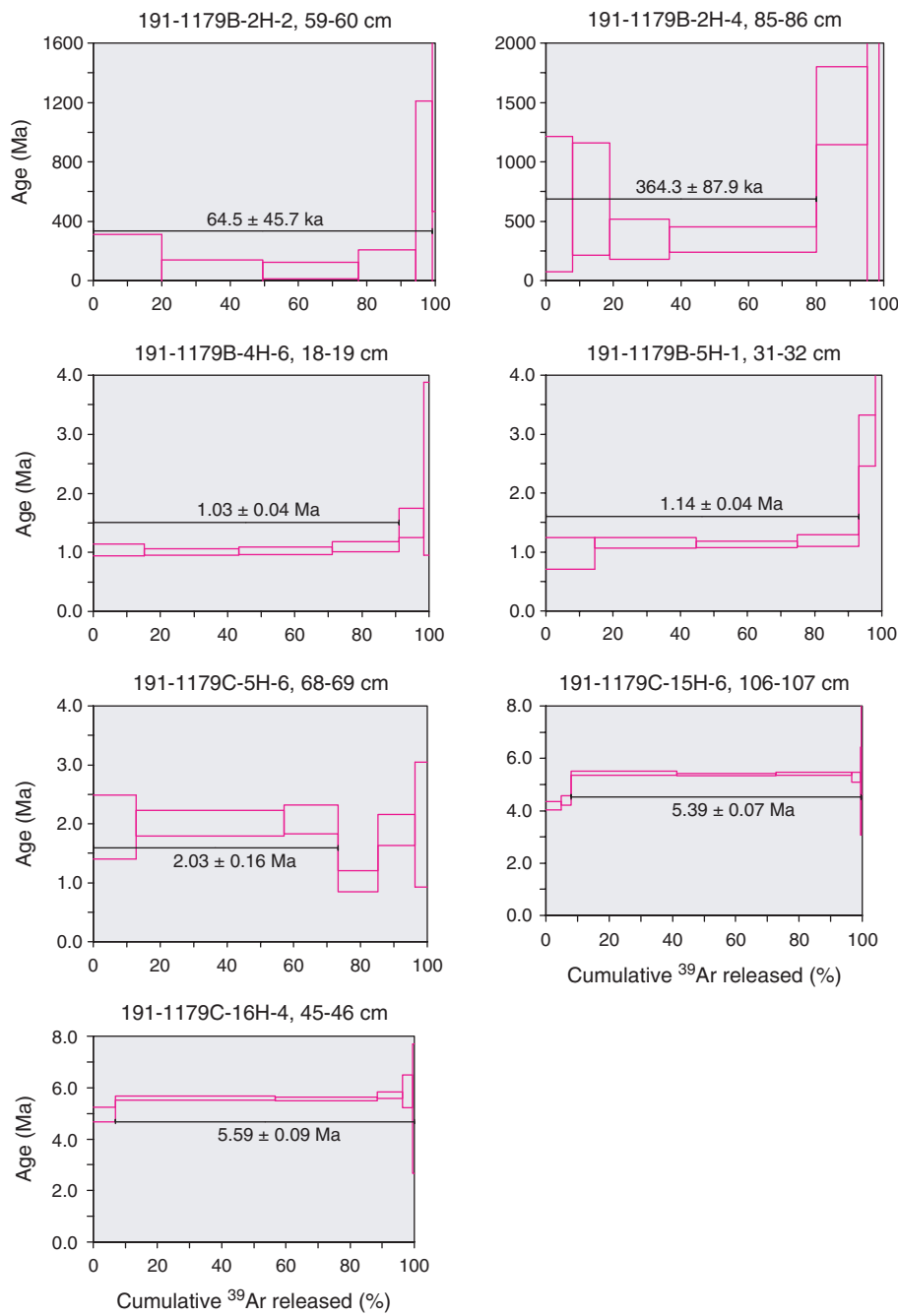


Figure F5. K/Ca ratio plots for Site 1179 samples.

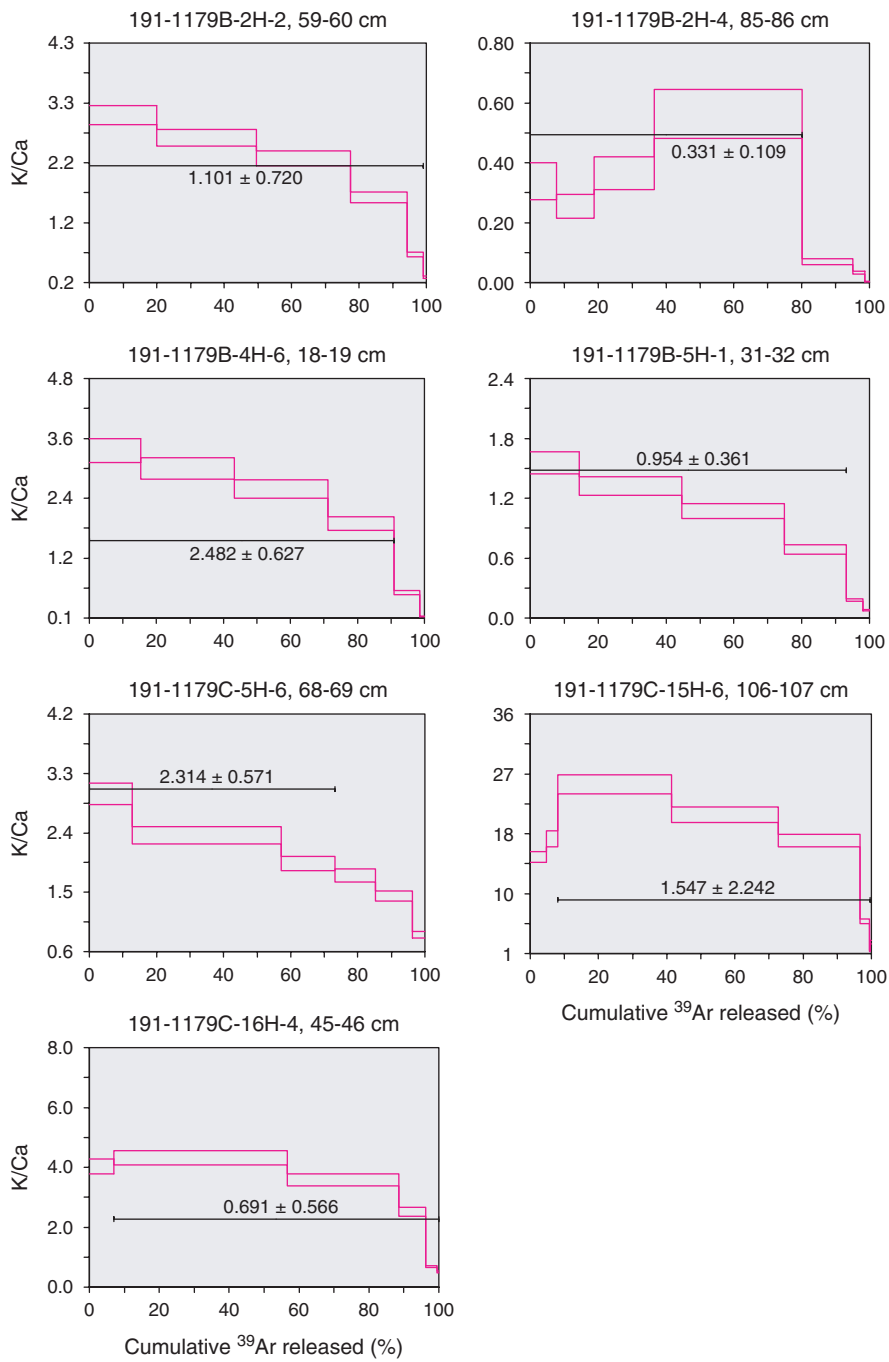


Figure F6. Age-depth plots for Sites 1149 and 1179 obtained with the refined combined $^{40}\text{Ar}/^{39}\text{Ar}$ chronology for the northwestern Pacific.

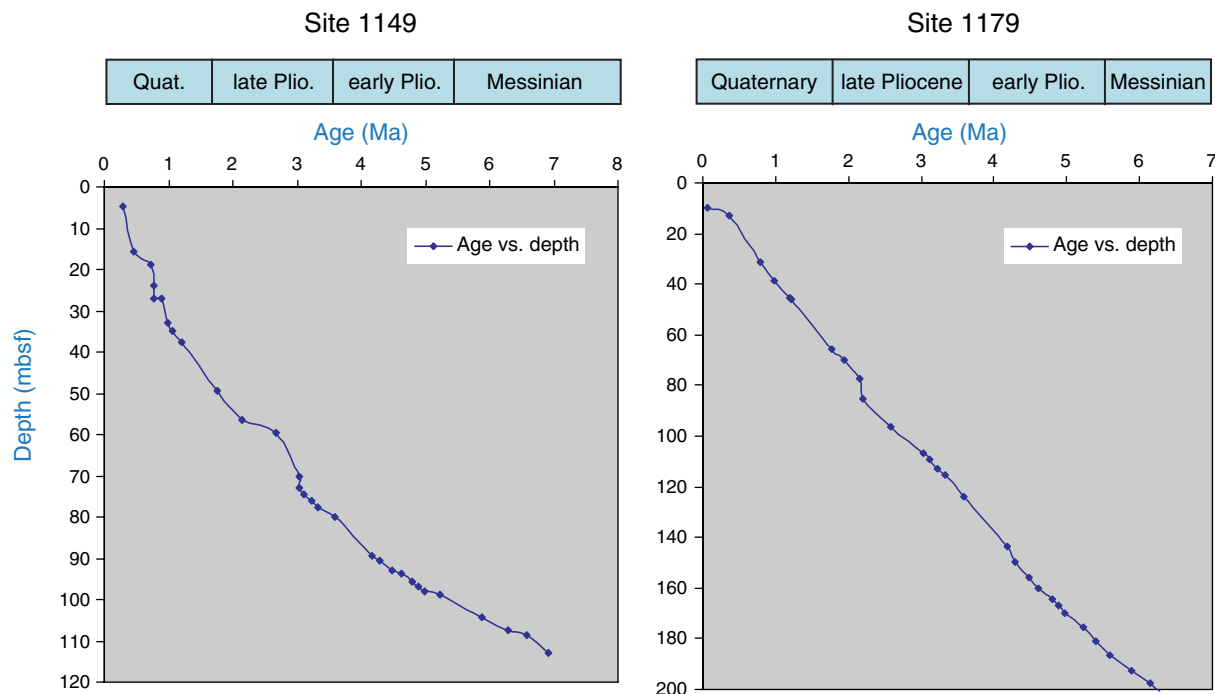


Table T1. Sample depth and age data for $^{40}\text{Ar}/^{39}\text{Ar}$ analysis, Site 1149.

Ages	Depth ($^{40}\text{Ar}/^{39}\text{Ar}$) (mbsf)	Age ($^{40}\text{Ar}/^{39}\text{Ar}$) (Ma)	Depth (paleo) (mbsf)	Age (paleo) (Ma)	Core depth (mbsf)	Core number
Quaternary	3.05	1.15 ± 0.20			185-1149A-	
	4.74	0.29 ± 0.04			1H	
	15.63	0.45 ± 0.08			4.2	2H
	18.75	0.71 ± 0.07			13.7	3H
	24.03	0.76 ± 0.08			23.2	4H
	27.16	0.89 ± 0.01	27.0	0.78		
					32.7	5H
				32.9	0.99	
				34.8	1.07	
				37.5	1.20	
Late Pliocene	50.68	1.58 ± 0.06			42.2	6H
	59.69	2.68 ± 0.03	52.7	1.95	51.7	7H
			56.5	2.14–2.15		
	70.17	3.03 ± 0.04	66.5	2.58	61.2	8H
					70.7	9H
				73.0	3.04	
				74.4	3.11	
				76.1	3.22	
				77.7	3.33	
				80.0	3.58	
Early Pliocene	85.5	5.41 ± 0.31			80.2	10H
			89.6	4.18		
					89.7	11H
			90.7	4.29		
			92.9	4.48		
			93.8	4.62		
			95.8	4.80		
			96.9	4.89		
			98.0	4.98		
			99.0	5.23		
Messinian	107.49	6.30 ± 0.06	99.2		99.2	12H
			104.4	5.89		
			108.6	6.56		
					108.7	13H
	112.85	6.92 ± 0.05				

Table T2. Sample depths and age data for $^{40}\text{Ar}/^{39}\text{Ar}$ analysis, Site 1179.

Ages	Depth ($^{40}\text{Ar}/^{39}\text{Ar}$) (mbsf)	Age ($^{40}\text{Ar}/^{39}\text{Ar}$) (Ma)	Depth (mag) (mbsf)	Age (mag) (Ma)	Core depth (mbsf)	Core number
Quaternary						
191-1179B-						
					1H	
			7.6		2H	
9.69	0.06 ± 0.04					
12.95	0.36 ± 0.09					
			31.12	0.78		
34.28	1.03 ± 0.04				17.1	3H
36.41	1.14 ± 0.04				26.6	4H
			38.57	0.99		
			45.6	1.20		
			45.92	1.21	45.6	6H
191-1179C-						
Late Pliocene						
		65.42	1.77		55.1	2H
					58.3	3H
		69.82	1.95		67.8	4H
		76.67	2.14			
		77.27	2.15			
				77.3	5H	
85.48	2.03 ± 0.16				86.8	6H
		96.17	2.58		96.3	7H
					105.8	8H
		106.52	3.04			
		109.42	3.11			
		112.72	3.22		115.3	9H
		115.52	3.33			
		123.77	3.58			
Early Pliocene						
			124.8	10H		
					134.3	11H
		143.80	4.18	143.8	12H	
		149.87	4.29			
				153.3	13H	
		155.92	4.48			
		160.02	4.62	162.8	14H	
		164.12	4.80			
		166.92	4.89			
		169.85	4.98			
Messinian						
			172.3	15H		
		175.72	5.23			
180.86	5.39 ± 0.07				181.8	16H
186.75	5.59 ± 0.09			191.3	17H	
		192.67	5.89			
		197.85	6.14			
		200.67	6.27			

Table T3. $^{40}\text{Ar}/^{39}\text{Ar}$ incremental heating data, Site 1149. (See table note. Continued on next page.)

Sample	Incremental heating ($^{\circ}\text{C}$)	^{36}Ar (a)	^{37}Ar (ca)	^{38}Ar (cl)	^{39}Ar (k)	^{40}Ar (r)	Age $\pm 2\sigma$ (Ma)	^{40}Ar (r) (%)	^{39}Ar (k) (%)	K/Ca $\pm 2\sigma$
185-1149A-										
1H-2, 55–56 cm	600	0.01830	0.29353	0.02798	0.17804	0.05238	0.84 ± 1.44	0.96	12.55	0.26 ± 0.01
	700	0.01395	0.59821	0.05932	0.27331	0.09237	0.96 ± 0.69	2.19	19.27	0.20 ± 0.01
	800	0.00925	1.00304	0.08686	0.35847	0.13060	1.04 ± 0.51	4.55	25.28	0.15 ± 0.01
	900	0.00644	1.25750	0.09415	0.37340	0.14123	1.08 ± 0.22	6.90	26.33	0.13 ± 0.01
	1000	0.00646	0.79502	0.03923	0.16637	0.08753	1.50 ± 0.43	4.38	11.73	0.09 ± 0.00
	1200	0.00791	0.52341	0.01294	0.06866	0.05319	2.21 ± 1.19	2.22	4.84	0.06 ± 0.00
	Σ	0.06232	4.47071	0.32047	1.41824	0.55729				
2H-1, 54–55 cm	600	0.00060	0.01740	0.00326	0.03532	0.00373	0.30 ± 0.63	2.07	1.66	0.87 ± 0.07
	700	0.00263	0.19465	0.03955	0.34609	0.04417	0.36 ± 0.20	5.36	16.30	0.76 ± 0.05
	800	0.00558	0.64604	0.12966	0.92288	0.09070	0.28 ± 0.07	5.19	43.47	0.61 ± 0.04
	900	0.00209	0.47046	0.08635	0.59096	0.06094	0.29 ± 0.04	8.90	27.83	0.54 ± 0.04
	1100	0.00357	0.23053	0.03228	0.21722	0.02374	0.31 ± 0.21	2.20	10.23	0.41 ± 0.03
	1400	0.00327	0.03891	0.00141	0.01076	0.01231	3.22 ± 3.49	1.26	0.51	0.12 ± 0.01
	Σ	0.01773	1.59799	0.29251	2.12323	0.23559				
3H-2, 43–44 cm	600	0.01315	0.25862	0.06106	0.50682	0.11206	0.61 ± 0.29	2.80	19.36	0.84 ± 0.04
	700	0.00438	0.17419	0.04235	0.26954	0.04216	0.43 ± 0.69	3.15	10.29	0.67 ± 0.04
	800	0.00989	0.77173	0.18447	0.99085	0.16421	0.46 ± 0.20	5.30	37.85	0.55 ± 0.03
	900	0.00639	0.59325	0.12447	0.65361	0.10114	0.43 ± 0.09	5.07	24.96	0.47 ± 0.03
	1000	0.00425	0.21627	0.03035	0.15827	0.02063	0.36 ± 0.52	1.62	6.05	0.31 ± 0.02
	1200	0.00364	0.13807	0.00531	0.03027	0.00886	0.81 ± 1.29	0.82	1.16	0.09 ± 0.01
	1400	0.00417	0.17992	0.00214	0.00879	0.02448	7.72 ± 4.37	1.95	0.34	0.02 ± 0.00
	Σ	0.04587	2.33205	0.45016	2.61816	0.47354				
3H-4, 55–56 cm	600	0.00209	0.11666	0.02420	0.81173	0.00000	0.00 ± 0.00	0.00	13.67	2.99 ± 0.17
	700	0.00338	0.27246	0.06012	1.73074	0.25091	0.43 ± 0.03	19.79	29.14	2.73 ± 0.15
	800	0.00303	0.25455	0.05419	1.40827	0.27047	0.58 ± 0.13	22.92	23.71	2.38 ± 0.13
	900	0.00319	0.22739	0.04480	1.10432	0.27939	0.76 ± 0.07	22.67	18.59	2.09 ± 0.12
	1000	0.00675	0.23367	0.02976	0.73587	0.17198	0.70 ± 0.11	7.91	12.39	1.35 ± 0.08
	1200	0.01200	0.26641	0.00496	0.12893	0.03145	0.73 ± 1.52	0.88	2.17	0.21 ± 0.01
	1400	0.00193	0.05038	0.00080	0.01927	0.01334	2.07 ± 2.34	2.29	0.32	0.16 ± 0.01
	Σ	0.03236	1.42154	0.21884	5.93914	1.01754				
4H-1, 89–90 cm	600	0.00527	0.07121	0.00847	0.24270	0.00900	0.10 ± 0.23	0.57	5.40	1.47 ± 0.10
	750	0.02004	0.88959	0.09358	2.18828	0.59455	0.74 ± 0.15	9.09	48.67	1.06 ± 0.06
	850	0.01124	0.80749	0.07790	1.65384	0.45897	0.76 ± 0.11	12.08	36.79	0.88 ± 0.05
	950	0.00713	0.30954	0.01516	0.32594	0.09625	0.81 ± 0.21	4.36	7.25	0.45 ± 0.03
	1100	0.01114	0.19511	0.00241	0.06359	0.04147	1.78 ± 1.90	1.24	1.41	0.14 ± 0.01
	1400	0.01281	0.16081	0.00185	0.02157	0.19493	24.54 ± 5.27	4.90	0.48	0.06 ± 0.00
	Σ	0.06763	2.43374	0.19937	4.49593	1.39517				
4H-3, 96–97 cm	600	0.00897	0.06787	0.01206	0.22177	0.07808	1.11 ± 0.44	2.86	4.87	1.40 ± 0.10
	700	0.03028	0.66796	0.14766	1.66811	0.46463	0.88 ± 0.18	4.93	36.60	1.07 ± 0.08
	800	0.00932	0.75937	0.15023	1.35757	0.38575	0.90 ± 0.17	12.24	29.79	0.77 ± 0.05
	900	0.00475	0.73155	0.11210	0.96876	0.26202	0.86 ± 0.18	15.64	21.26	0.57 ± 0.04
	1050	0.00561	0.44182	0.03694	0.31569	0.13053	1.31 ± 0.20	7.29	6.93	0.31 ± 0.02
	1400	0.00814	0.15541	0.00261	0.02564	0.05761	7.10 ± 4.60	2.34	0.56	0.07 ± 0.01
	Σ	0.06707	2.82398	0.46159	4.55753	1.37862				
6H-1, 98–99 cm	600	0.00900	0.62888	0.04820	2.03660	1.05811	1.61 ± 0.11	28.31	26.32	1.39 ± 0.22
	750	0.00635	0.53931	0.09225	3.51735	1.76900	1.56 ± 0.03	48.06	45.46	2.80 ± 0.40
	850	0.01119	0.00000	0.05861	2.04711	1.11145	1.68 ± 0.10	25.03	26.46	0.57 ± 0.00
	950	0.01650	0.00000	0.00271	0.08500	0.49418	17.94 ± 3.27	9.20	1.10	0.00 ± 0.00
	1100	0.01130	0.00000	0.00105	0.03932	0.30965	24.26 ± 8.42	8.48	0.51	0.00 ± 0.00
	1400	0.00272	0.67348	0.00016	0.01109	0.32328	88.24 ± 7.85	28.70	0.14	0.01 ± 0.00
	Σ	0.05706	1.84167	0.20297	7.73646	5.06567				
7H-7, 49–50 cm	500	0.05500	0.28034	0.01523	0.48812	0.34393	2.13 ± 2.92	2.07	5.42	0.75 ± 0.13
	600	0.01574	0.59851	0.04340	1.47453	1.32324	2.72 ± 0.35	22.09	16.36	1.06 ± 0.17
	675	0.01040	0.40482	0.03944	1.24274	1.10130	2.68 ± 0.13	26.31	13.79	1.32 ± 0.21
	750	0.00616	0.44137	0.09347	2.84232	2.50857	2.67 ± 0.04	57.58	31.54	2.77 ± 0.42
	800	0.00249	0.23934	0.05352	1.61064	1.43552	2.70 ± 0.05	65.65	17.87	2.89 ± 0.49
	850	0.00288	0.29189	0.02971	0.86647	0.85649	2.99 ± 0.07	49.91	9.62	1.28 ± 0.22
	950	0.00597	0.13365	0.01104	0.33078	0.40636	3.72 ± 0.26	18.70	3.67	1.06 ± 0.28
	1100	0.01381	0.21916	0.00331	0.09946	0.55413	16.81 ± 2.33	11.96	1.10	0.20 ± 0.03
	1400	0.00390	0.26688	0.00070	0.05569	0.73018	39.30 ± 1.51	38.80	0.62	0.09 ± 0.01
	Σ	0.11633	2.87598	0.28983	9.01077	9.25971				
8H-6, 147–148 cm	500	0.01420	0.25136	0.00596	0.28056	0.27670	3.02 ± 0.71	6.18	3.46	0.48 ± 0.11
	600	0.03968	0.67058	0.02827	1.32358	1.31522	3.05 ± 0.53	10.07	16.31	0.85 ± 0.17
	675	0.03810	0.55925	0.03684	1.65804	1.63118	3.01 ± 0.32	12.64	20.43	1.27 ± 0.21
	750	0.00997	0.22016	0.02704	1.14426	1.09595	2.94 ± 0.12	27.03	14.10	2.23 ± 0.45

Table T3 (continued).

Sample	Incremental heating ($^{\circ}\text{C}$)	^{36}Ar (a)	^{37}Ar (ca)	^{38}Ar (cl)	^{39}Ar (k)	^{40}Ar (r)	Age $\pm 2\sigma$ (Ma)	^{40}Ar (r) (%)	^{39}Ar (k) (%)	K/Ca $\pm 2\sigma$
	825	0.00358	0.14572	0.02748	1.21598	1.20517	3.04 ± 0.05	52.99	14.98	3.59 ± 0.97
	900	0.01398	0.23222	0.05240	2.30432	2.30370	3.06 ± 0.08	35.67	28.39	4.27 ± 0.92
	975	0.01591	0.04376	0.00383	0.14525	0.14060	2.97 ± 1.57	2.90	1.79	1.43 ± 1.19
	1100	0.01974	0.02803	0.00196	0.03293	0.10567	9.82 ± 9.10	1.78	0.41	0.51 ± 0.25
	1400	0.00383	0.07904	0.00045	0.01160	0.08224	21.61 ± 4.88	6.78	0.14	0.06 ± 0.03
	Σ	0.15899	2.23011	0.18424	8.11652	8.15644				
10H-5, 80–81 cm	500	0.04872	0.21630	0.05801	0.42131	0.46895	3.33 ± 1.36	3.15	5.39	0.84 ± 0.20
	600	0.03469	0.58583	0.11187	1.56960	2.45847	4.68 ± 0.34	19.32	20.08	1.15 ± 0.20
	675	0.01594	0.44989	0.09865	2.04964	3.65093	5.32 ± 0.11	43.55	26.22	1.96 ± 0.40
	750	0.01864	0.24937	0.10504	1.98386	3.75398	5.65 ± 0.13	40.45	25.37	3.42 ± 0.68
	800	0.00482	0.07373	0.02647	0.85225	1.75397	6.15 ± 0.09	55.03	10.90	4.97 ± 2.21
	875	0.00568	0.00000	0.01688	0.74897	1.61764	6.45 ± 0.11	48.99	9.58	0.00 ± 0.00
	1000	0.01111	0.00000	0.00353	0.13309	0.36722	8.23 ± 1.09	10.05	1.70	0.00 ± 0.00
	1400	0.01436	0.33990	0.00187	0.05973	0.49307	24.52 ± 3.32	10.41	0.76	0.08 ± 0.01
	Σ	0.15396	1.91501	0.42233	7.81845	14.56423				
12H-6, 79–80 cm	500	0.00301	0.11821	0.00273	0.06511	0.13725	6.59 ± 0.79	13.37	1.40	0.24 ± 0.07
	650	0.01357	0.76918	0.05905	1.36457	2.75470	6.32 ± 0.19	40.64	29.27	0.76 ± 0.12
	700	0.00726	0.73139	0.06705	1.31950	2.65163	6.29 ± 0.08	55.14	28.30	0.78 ± 0.12
	750	0.00226	0.45542	0.02288	0.41084	0.82571	6.29 ± 0.14	55.12	8.81	0.39 ± 0.07
	825	0.00521	0.51624	0.05604	0.96438	1.94963	6.32 ± 0.11	55.73	20.69	0.80 ± 0.13
	900	0.00402	0.17823	0.01479	0.27391	0.55356	6.32 ± 0.21	31.72	5.88	0.66 ± 0.15
	1100	0.01538	0.25703	0.00414	0.18609	0.57338	9.63 ± 1.19	11.20	3.99	0.31 ± 0.06
	1400	0.01107	0.43597	0.00159	0.07758	0.35699	14.36 ± 2.07	9.84	1.66	0.08 ± 0.01
	Σ	0.06177	3.46167	0.22828	4.66198	9.80286				
13H-3, 115–116 cm	500	0.00313	0.09497	0.00213	0.13416	0.26381	6.22 ± 0.53	22.18	1.42	0.61 ± 0.18
	600	0.02563	0.40813	0.05318	3.35209	7.33794	6.92 ± 0.12	49.10	35.48	3.53 ± 0.56
	675	0.00846	0.44628	0.04514	2.79292	6.15942	6.97 ± 0.05	70.91	29.56	2.69 ± 0.45
	750	0.00672	0.30031	0.03885	2.29515	5.00058	6.89 ± 0.06	71.34	24.29	3.29 ± 0.62
	825	0.00437	0.16055	0.00870	0.52055	1.12852	6.85 ± 0.13	46.55	5.51	1.39 ± 0.24
	950	0.01120	1.07819	0.00213	0.20842	0.45821	6.95 ± 0.86	12.16	2.21	0.08 ± 0.01
	1100	0.00803	0.17091	0.00109	0.12518	0.33737	8.51 ± 0.85	12.45	1.32	0.31 ± 0.06
	1400	0.00023	3.27601	0.00026	0.01962	0.30638	48.77 ± 6.17	81.58	0.21	0.00 ± 0.00
	Σ	0.06775	5.93535	0.15148	9.44810	20.99223				

Note: a = atmospheric, ca = neutron interaction on calcium, cl = neutron interaction on chlorine, k = neutron interaction on potassium, r = radiogenic.

Table T4. $^{40}\text{Ar}/^{39}\text{Ar}$ incremental heating data, Site 1179.

Sample	Incremental heating ($^{\circ}\text{C}$)	^{36}Ar (a)	^{37}Ar (ca)	^{38}Ar (cl)	^{39}Ar (k)	^{40}Ar (r)	Age $\pm 2\sigma$ (Ma)	^{40}Ar (r) (%)	^{39}Ar (k) (%)	K/Ca $\pm 2\sigma$
191-1179B-										
2H-2, 59–60 cm	600	0.01618	0.21037	0.06147	1.48818	0.03680	0.08 ± 0.23	0.76	20.07	3.042 ± 0.162
	700	0.01246	0.35450	0.10985	2.19217	0.02779	0.04 ± 0.10	0.74	29.57	2.659 ± 0.142
	800	0.00928	0.38345	0.11322	2.06693	0.04449	0.07 ± 0.06	1.58	27.88	2.318 ± 0.125
	900	0.00958	0.32332	0.06973	1.24591	0.02762	0.07 ± 0.14	0.96	16.81	1.657 ± 0.090
	1100	0.02339	0.22294	0.01832	0.35814	0.06081	0.53 ± 0.68	0.87	4.83	0.691 ± 0.037
	1400	0.00681	0.08664	0.00319	0.06203	0.02902	1.47 ± 0.01	1.42	0.84	0.308 ± 0.017
	Σ	0.07770	1.5812	0.3758	7.4134	0.22654				
2H-4, 85–86 cm	500	0.00484	0.26322	0.01893	0.20677	0.04172	0.65 ± 0.57	2.83	7.79	0.338 ± 0.061
	600	0.00334	0.49501	0.03179	0.29334	0.06301	0.69 ± 0.47	5.98	11.06	0.255 ± 0.040
	700	0.00378	0.55478	0.06473	0.47079	0.05109	0.35 ± 0.17	4.35	17.75	0.365 ± 0.055
	800	0.00654	0.88127	0.17406	1.15381	0.12435	0.34 ± 0.11	6.01	43.49	0.563 ± 0.081
	900	0.00421	2.46312	0.05904	0.39742	0.18299	1.47 ± 0.33	12.78	14.98	0.069 ± 0.010
	1050	0.01337	1.25764	0.00948	0.09470	0.04996	1.69 ± 2.12	1.25	3.57	0.032 ± 0.005
	1400	0.01895	4.57488	0.00403	0.03610	0.29987	26.37 ± 9.70	5.08	1.36	0.003 ± 0.000
	Σ	0.05504	10.48992	0.36207	2.65294	0.81298				
4H-6, 18–19 cm	600	0.01742	0.21779	0.06141	1.69428	0.57298	1.04 ± 0.10	9.98	15.23	3.345 ± 0.236
	700	0.01705	0.44883	0.13685	3.12660	1.02429	1.01 ± 0.06	16.81	28.10	2.995 ± 0.212
	800	0.01192	0.51401	0.14943	3.09683	1.03298	1.03 ± 0.06	22.53	27.83	2.591 ± 0.183
	900	0.01093	0.49432	0.10946	2.20778	0.78582	1.10 ± 0.08	19.46	19.84	1.921 ± 0.136
	1100	0.02325	0.63953	0.03909	0.83561	0.40647	1.50 ± 0.25	5.58	7.51	0.562 ± 0.040
	1400	0.02049	0.77127	0.01453	0.16559	0.13029	2.42 ± 1.47	2.11	1.49	0.092 ± 0.007
	Σ	0.10106	3.08574	0.51077	11.12669	3.95283				
5H-1, 31–32 cm	600	0.01325	0.23928	0.04078	0.86445	0.27129	0.98 ± 0.27	6.46	14.45	1.553 ± 0.109
	700	0.01396	0.58724	0.11612	1.80744	0.66909	1.15 ± 0.09	13.90	30.22	1.323 ± 0.093
	800	0.00877	0.72368	0.13073	1.80200	0.65276	1.13 ± 0.05	20.01	30.13	1.071 ± 0.075
	900	0.00728	0.68550	0.08108	1.09704	0.42014	1.19 ± 0.10	16.27	18.34	0.688 ± 0.048
	1100	0.00972	0.70823	0.01746	0.29517	0.27389	2.89 ± 0.44	8.70	4.94	0.179 ± 0.013
	1400	0.01260	0.63988	0.00589	0.11435	0.37633	10.23 ± 1.44	9.18	1.91	0.077 ± 0.005
	Σ	0.06558	3.58381	0.39207	5.98044	2.66350				
191-1179C-										
5H-6, 68–69 cm	600	0.04439	0.11766	0.04221	0.82497	0.52883	1.94 ± 0.54	3.87	12.88	3.015 ± 0.162
	700	0.05602	0.51084	0.18702	2.83687	1.88083	2.01 ± 0.22	10.19	44.28	2.388 ± 0.130
	750	0.01042	0.22571	0.08582	1.02841	0.70519	2.08 ± 0.24	18.58	16.05	1.959 ± 0.107
	800	0.00805	0.18683	0.06889	0.77387	0.26075	1.02 ± 0.18	9.85	12.08	1.781 ± 0.097
	900	0.00855	0.20722	0.06448	0.70832	0.44281	1.89 ± 0.26	14.87	11.05	1.470 ± 0.079
	1100	0.01429	0.11411	0.01784	0.23485	0.15371	1.98 ± 1.06	3.51	3.67	0.885 ± 0.048
	Σ	0.14172	1.36238	0.46626	6.40727	3.97211				
15H-6, 106–107 cm	500	0.00792	0.01815	0.02694	0.62547	0.88958	4.19 ± 0.15	27.50	4.75	14.820 ± 0.792
	600	0.00405	0.01043	0.01821	0.42389	0.63182	4.39 ± 0.18	34.48	3.22	17.481 ± 1.179
	700	0.01628	0.07427	0.20272	4.39382	8.10870	5.44 ± 0.07	62.55	33.38	25.438 ± 1.376
	800	0.00836	0.08457	0.20510	4.13931	7.55214	5.38 ± 0.04	75.03	31.45	21.047 ± 1.130
	900	0.00757	0.07843	0.16329	3.14131	5.76450	5.41 ± 0.05	71.77	23.87	17.222 ± 0.939
	1000	0.00478	0.02786	0.01874	0.35788	0.64044	5.27 ± 0.19	31.16	2.72	5.524 ± 0.343
	1100	0.00387	0.01192	0.00110	0.03167	0.05104	4.75 ± 1.68	4.27	0.24	1.143 ± 0.071
	1400	0.00246	0.00852	0.00165	0.04801	0.11566	7.10 ± 2.48	13.72	0.36	2.423 ± 0.248
	Σ	0.05528	0.31415	0.63775	13.16136	23.75388				
16H-4, 45–46 cm	600	0.00840	0.05139	0.01308	0.48158	0.82468	4.96 ± 0.29	24.89	6.98	4.030 ± 0.254
	700	0.02021	0.34139	0.09416	3.42684	6.62278	5.60 ± 0.08	52.44	49.70	4.316 ± 0.244
	800	0.00982	0.26342	0.06709	2.19690	4.21840	5.56 ± 0.06	59.06	31.86	3.586 ± 0.202
	900	0.00421	0.09122	0.01746	0.53272	1.04922	5.70 ± 0.13	45.64	7.73	2.511 ± 0.147
	1100	0.01253	0.13537	0.00566	0.21586	0.43642	5.86 ± 0.65	10.54	3.13	0.686 ± 0.039
	1400	0.00726	0.03436	0.00088	0.04076	0.07298	5.19 ± 2.51	3.29	0.59	0.510 ± 0.029
	Σ	0.06242	0.91715	0.19834	6.89465	13.22448				

Note: a = atmospheric, ca = neutron interaction on calcium, cl = neutron interaction on chlorine, k = neutron interaction on potassium, r = radiogenic.

Table T5. New combined $^{40}\text{Ar}/^{39}\text{Ar}$ and magnetostratigraphic chronostratigraphy.

Site	Depth (mbsf)	Age (Ma)
1149	4.74	0.29 ± 0.04
	15.63	0.45 ± 0.08
	18.75	0.71 ± 0.07
	24.03	0.76 ± 0.08
	27.00	0.78
	27.16	0.89 ± 0.01
	32.90	0.99
	34.80	1.07
	37.50	1.2
	49.60	1.77
	52.70	1.95
	56.50	2.14–2.15
	66.50	2.58
	70.17	3.03 ± 0.04
	73.00	3.04
	74.40	3.11
	76.10	3.22
	77.70	3.33
	80.00	3.58
	89.60	4.18
	90.70	4.29
	92.90	4.48
	93.80	4.62
	95.80	4.8
	96.90	4.89
	98.00	4.98
	99.00	5.23
	104.40	5.89
	107.49	6.30 ± 0.06
	108.60	6.57
	112.85	6.92 ± 0.05
1179	9.69	0.06 ± 0.04
	12.95	0.36 ± 0.09
	31.12	0.78
	38.57	0.99
	45.60	1.2
	45.92	1.21
	65.42	1.77
	69.82	1.95
	76.67	2.14
	77.27	2.15
	96.17	2.58
	106.52	3.04
	109.42	3.11
	112.72	3.22
	115.52	3.33
	123.77	3.58
	143.80	4.18
	149.87	4.29
	155.92	4.48
	160.02	4.62
	164.12	4.8
	166.92	4.89
	169.85	4.98
	175.72	5.23
	180.86	5.39 ± 0.07
	186.75	5.59 ± 0.09
	192.67	5.89
	197.85	6.13
	200.67	6.27